RSC Advances

PAPER

View Article Online
View Journal | View Issue

Cite this: *RSC Adv.*, 2019, **9**, 3577

New high-pressure phases of Fe_7N_3 and Fe_7C_3 stable at Earth's core conditions: evidences for carbon–nitrogen isomorphism in Fe-compounds†

Nursultan Sagatov, *[ab] Pavel N. Gavryushkin, [ab] Talgat M. Inerbaev[ac] and Konstantin D. Litasov[ab]

Received 3rd December 2018
Accepted 15th January 2019

DOI: 10.1039/c8ra09942a

rsc.li/rsc-advances

We carried out *ab initio* calculations on the crystal structure prediction and determination of *P*–*T* diagrams within the quasi-harmonic approximation for Fe_7N_3 and Fe_7C_3. Two new isostructural phases Fe_7N_3-*C*2/*m* and Fe_7C_3-*C*2/*m* which are dynamically and thermodynamically stable under the Earth's core conditions were predicted. The Fe_7C_3-*C*2/*m* phase stabilizes preferentially to the known h-Fe_7C_3 at 253–344 GPa in the temperature range of 0–5000 K, and the Fe_7N_3-*C*2/*m* stabilizes preferentially relative to the β-Fe_7N_3 – at ∼305 GPa over the entire temperature range. This indicate that carbon and nitrogen can mutually coexist and replace each other in the Earth's and other planetary cores similarly to low pressure phases of the same compounds.

1. Introduction

Iron carbides' and nitrides' behaviour at high pressures is important due to the close correspondence of the density and elastic properties of these compounds to those of the Earth's core.[2] Carbides are classical candidates for the list of the Earth's core potential phases,[3,4] while nitrides are newcomers in this list. The uprising interest to iron nitrides is due to their recent findings in meteorites and deep mantle rocks.[6–9]

Fe_7C_3 and Fe_7N_3 stoichiometries are considered as potential inner core constituents among known Fe–C and Fe–N compounds. In the case of Fe_7C_3, this assumption is based on the experimental results, showing that this compound crystallizes first from the iron melt at pressures of 130 GPa, and also on the close correspondence of its density to that of the Earth's core.[10–12] In the case of Fe_7N_3, the assumption is based on the greater stability of Fe_7N_3 compared to the other nitrides under the inner core conditions.[13,14]

Fe_7C_3 iron carbide presents in the form of two modifications: low-pressure orthorhombic o-Fe_7C_3 (*Pbca*) and high-pressure hexagonal h-Fe_7C_3 ($P6_3mc$). o-Fe_7C_3 was synthesized in the pressure range of 7–15 GPa with heating to about 2000 K, and was traced up to pressures of ∼205 GPa and temperatures above 3700 K.[15] Based on the results, the authors assumed the stability of o-Fe_7C_3 under the conditions of the Earth's inner core. In contrast, the calculations within the density functional theory (DFT) show that at 0 K transition from o- to h-phase takes place at ∼100 GPa.[16,17] The equation of state of the h-phase was experimentally determined up to 71 GPa and 1973 K,[11] and theoretically – up to 364 GPa at 0 K.[18] In the same work, the disappearance of the magnetic moment was predicted at pressures near 67 GPa. The close correspondence of the h-phase elastic properties and those of PREM (preliminary reference Earth model)[5] at 350 GPa and 6500 K was shown with molecular dynamic simulations.[19] However, the obtained density is significantly lower than that of PREM. With evolutionary crystal structure prediction method, which we also applied here, it was shown that the h-Fe_7C_3 phase is the most energetically favourable modification in the pressure range of 100–400 GPa at 0 K.[20]

Fe_7N_3 was synthesized in the form of the low-pressure ε- and high-pressure β-phases.[14,21,22] The ε-phase transforms into the β-phase at 41 GPa and 1000 K, which remains stable at least up to 132 GPa.[14] Crystal structure of β-phase has not been determined experimentally. However, based on the similarity of its powder diffraction pattern to that of h-Fe_7C_3, the conclusion about similarity of their structures has been inferred. With DFT calculations we have confirmed this conclusion, shown that β-Fe_7N_3 (isostructural to h-Fe_7C_3) became more favourable than ε-phase at pressures above 67 GPa at 0 K.[23] In the same work we also found the new phase Fe_7N_3-*Amm*2, which is energetically more favourable than the β-phase in the pressure range of 43–128 GPa at 0 K. The apparent difference between the experimental and theoretical stability fields of the β- and *Amm*2-phases was explained by the kinetic effects, preventing transformation of high-temperature β-phase to the low-temperature *Amm*2-phase.

In the present study, we show the results of *ab initio* determination of Fe_7N_3 and Fe_7C_3 phase diagrams at pressures up to

[a]*Sobolev Institute of Geology and Mineralogy, Siberian Branch of the Russian Academy of Sciences, Novosibirsk, 630090 Russia. E-mail: sagatinho23@gmail.com*
[b]*Novosibirsk State University, Novosibirsk, 630090 Russia*
[c]*L. N. Gumilyov Eurasian National University, Astana, 010008 Kazakhstan*

† Electronic supplementary information (ESI) available: Method of quasi-harmonic approximation, phonon dispersion curves, structures predicted by USPEX and AIRSS method. See DOI: 10.1039/c8ra09942a

Table 1 Structural data for the predicted phases of Fe_7N_3 and Fe_7C_3

Phase	Pressure (GPa)	Space group	Lattice parameters (Å, degree)			Atomic coordinates			
						Atom	x	y	z
β-Fe_7N_3	150	$P6_3mc$ (#186)	$a = 6.1895$	$b = 6.1895$	$c = 4.0302$	Fe1	0.87626	0.12374	0.09945
						Fe2	0.54300	0.45700	0.77221
			$\alpha = 90.00$	$\beta = 90.00$	$\gamma = 120.00$	Fe3	0.33333	0.66667	0.75557
						N1	0.18882	0.81117	0.00704
Fe_7N_3-$Cmc2_1$	300	$Cmc2_1$ (#36)	$a = 14.1246$	$b = 4.0580$	$c = 4.1031$	Fe1	0.13011	0.43015	0.09662
						Fe2	0.07758	0.07317	0.46654
						Fe3	0.22858	0.15317	0.38888
			$\alpha = 90.00$	$\beta = 90.00$	$\gamma = 90.00$	Fe4	0.00000	0.38436	0.79986
						N1	0.16249	0.18579	0.76342
						N2	0.00000	0.78323	0.67610
Fe_7N_3-$C2/m$	400	$C2/m$ (#12)	$a = 7.4226$	$b = 2.1497$	$c = 7.1380$	Fe1	0.80328	0.00000	0.89918
						Fe2	0.04345	0.00000	0.80958
						Fe3	0.31221	0.00000	0.63162
			$\alpha = 90.00$	$\beta = 106.0204$	$\gamma = 90.00$	Fe4	0.00000	0.00000	0.50000
						N1	0.64161	0.00000	0.67115
						N2	0.00000	0.50000	0.00000
Fe_7C_3-$C2/m$	400	$C2/m$ (#12)	$a = 7.3888$	$b = 2.1581$	$c = 7.0895$	Fe1	0.80215	0.00000	0.89823
						Fe2	0.04461	0.00000	0.81018
						Fe3	0.31877	0.00000	0.63295
			$\alpha = 90.00$	$\beta = 104.9195$	$\gamma = 90.00$	Fe4	0.00000	0.00000	0.50000
						C1	0.64452	0.00000	0.66454
						C2	0.00000	0.50000	0.00000

the Earth's inner core conditions, *i.e.* 350 GPa and 6000 K, illustrating crystallochemical similarity of these compounds and described new crystal structure, which are potentially applicable for the phases stable in the Earth's inner core.

2. Computational details

The calculations were performed using two structure prediction codes based on fundamentally different approaches: USPEX[24–27] based on evolutionary algorithms and AIRSS[28,29] based on a random sampling method. Both methods show their effectiveness in predicting crystal structures of inorganic compounds,[30–33] including carbides and nitrides.[20,23,34]

The calculations of the electronic structure were carried out within the DFT using the VASP 5.3 package.[35–37] The exchange–correlation interaction was taken into account in the generalized gradient approximation (GGA) in the form of the Perdew–Burke–Ernzerhof (PAW) functional.[38] Since the recent theoretical[16,18,23] and experimental[12,15] results showed that for iron carbides and nitrides, the disappearance of the magnetic moment occurs at pressures below 100 GPa, we performed non spin-polarized calculations above this pressure.

The crystal structure prediction calculations (by both USPEX and AIRSS) were performed for Fe_7N_3 and Fe_7C_3 stoichiometries. For each compound, we performed calculations for two formula units and 150, 200, 300 and 400 GPa. The size of the first generation in the calculations with USPEX code was equal to 30 structures. 60% of the structures with the lowest enthalpy were selected after the optimization and then used for producing the next generation (40% – by heredity, 20% – by atomic mutation, 10% – by lattice permutation, and 30% – randomly). Using AIRSS 900–1100 structures were randomly generated and optimized and those with the lowest enthalpy were selected. The atomic positions were optimized within the DFT for the structures obtained with both prediction methods. The computation parameters were as follows: energy cut-off – 450 eV; the density of the grid of Monkhorst–Pack k-point mesh[39] – 0.5 $Å^{-1}$; electronic smearing – with Methfessel-Paxton scheme;[40] parameter $\sigma = 0.05$ eV. The most promising predicted structures were then optimized with higher accuracy at various pressures. In these calculations, the cut-off energy was 600 eV, the density of k-points was 0.2 $Å^{-1}$, and parameter $\sigma = 0.01$ eV.

To take into account the temperature effect and predict the phase diagrams, we used the method of lattice dynamics within the quasi-harmonic approximation (QHA). For this task, the phonon frequencies were calculated with the PHONOPY code.[41] The energy cut-off in this case has been increased to 800 eV (for the details of the method see the ESI†).

3. Results and dicussion

3.1 Iron nitride Fe_7N_3

The comparison of crystal structure predictions by USPEX and AIRSS methods are summarized in Table S1 in the ESI,† whereas structural data of the new phases – in Table 1. At 150,

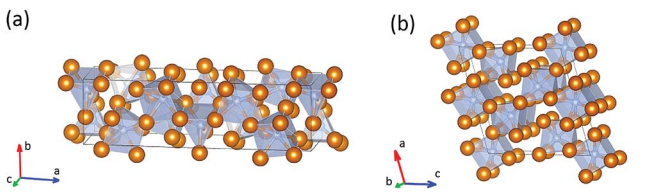

Fig. 1 Structural models of Fe_7N_3-$Cmc2_1$ (a) and -$C2/m$ (b). The brown balls correspond to iron atoms, blue balls – to nitrogen atoms.

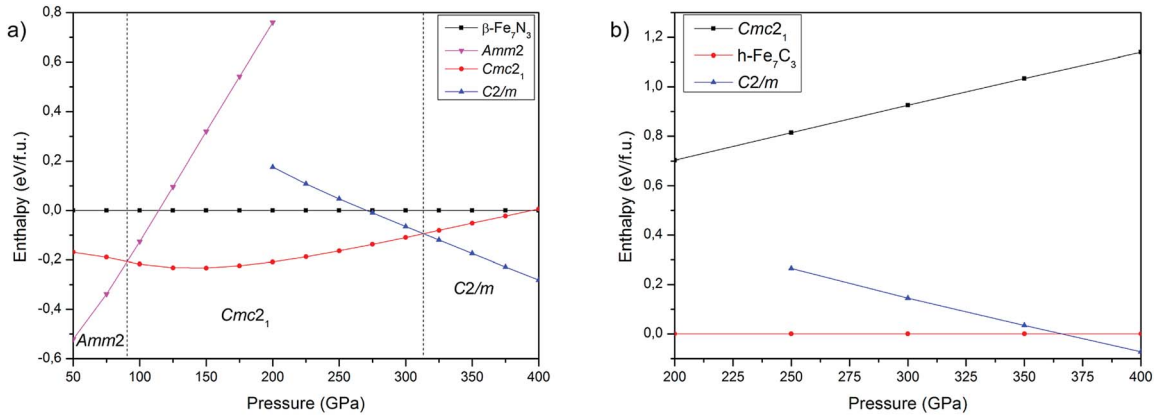

Fig. 2 Pressure dependencies of the enthalpy for Fe_7N_3 (a) and Fe_7C_3 (b).

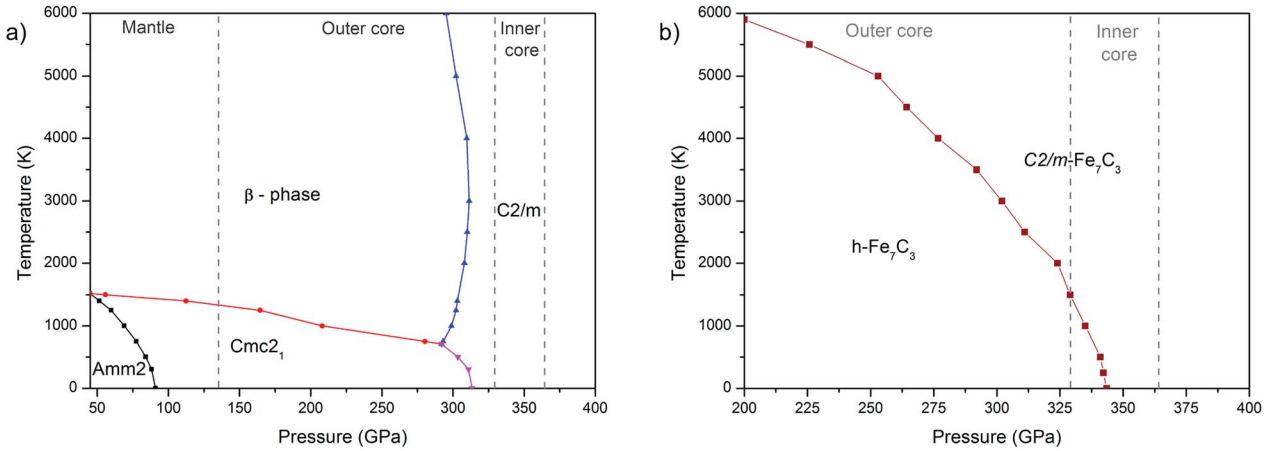

Fig. 3 *P*–*T* phase diagrams of Fe_7N_3 (a) and Fe_7C_3 (b).

200 and 300 GPa, both methods revealed preferential stability of the experimentally synthesized phase β-Fe_7N_3 ($P6_3mc$) and a new structure $Cmc2_1$. However, at 400 GPa the results of predictions are different. USPEX found the new $C2/m$ structure as the most favourable, while AIRSS found $Cmc2_1$. Thus, in case of Fe_7N_3 compound USPEX algorithms show higher efficiency in revealing of energetically favourable structures. The same was observed for iron carbides.[20]

At 300 GPa the density of Fe_7N_3-$C2/m$ is ~1% higher than the density of $Cmc2_1$ phase. The density difference can be explained by differences in coordination numbers. In the structure of the $C2/m$ phase carbon is in the seven- and eightfold coordinations by iron with one-cap trigonal prism and cube as coordination polyhedrons. In the less dense $Cmc2_1$ phase – in the six- and sevenfold coordinations, with trigonal prism and the one-cap trigonal prism as coordination polyhedrons (Fig. 1).

The calculated dependencies of enthalpy on pressure at 0 K (Fig. 2a) show that *Amm*2 phase is energetically favorable in the low-pressure region. At 90 GPa *Amm*2 phase transforms to the $Cmc2_1$, which in turn transforms to the $C2/m$ at 313 GPa. The β-phase is metastable over the entire pressure range. As noted above, β-phase was synthesized at 41 GPa and 1000 K and remains stable up to 132 GPa and 2500 K. To resolve this inconsistency between computations and experimental results we constructed phonon spectra and performed the Gibbs free energy calculations. The phonon spectra confirmed the dynamic stability of all predicted phases, with the exception of

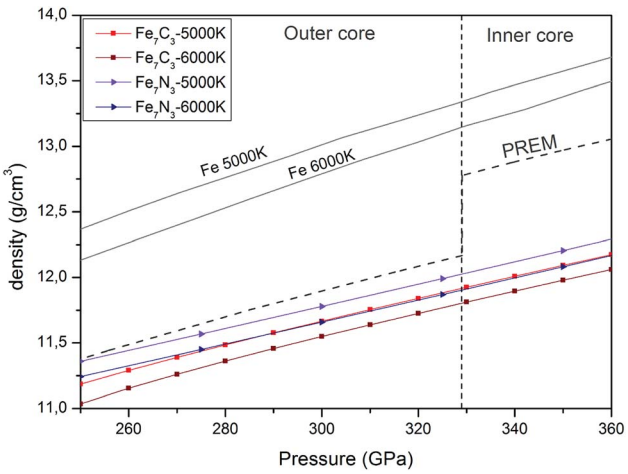

Fig. 4 Pressure and density profiles of Fe_7N_3-$C2/m$, Fe_7C_3-$C2/m$ and hcp-Fe[1] in comparison with PREM model[5] under the Earth's core conditions.

Table 2 Comparison of the density of Fe_7N_3-*C*2/*m* and Fe_7C_3-*C*2/*m* with Preliminary Reference Earth Model (PREM)[5] and hcp-Fe[1]

Phase	Temperature, K	$\rho_{329\ GPa}$, g cm^{-3}	$\rho_{364\ GPa}$, g cm^{-3}	(C, N), wt%
PREM		12.76	13.09	
Fe_7N_3-*C*2/*m*	5000	12.025	12.33	4.0–4.1
	6000	11.903	12.202	2.8–3.0
Fe_7C_3-*C*2/*m*	5000	11.917	12.21	3.2–3.3
	6000	11.803	12.095	2.2–2.4
hcp-Fe	5000	13.34	13.72	
	6000	13.14	13.53	

the β-Fe_7N_3 phase, which phonon spectrum is characterized by small negative frequencies in the region of the *Γ*-point (Fig. S1 in the ESI†).

The calculated *P*–*T* phase diagram (Fig. 3a) explains synthesis of β-phase in the experiment. According to the diagram *Amm*2 and *Cmc*2_1 are low-temperature phases, which on heating above 1000–1500 K transform into the β-phase. Due to a significant structural difference between the *Amm*2 and β-phases, in the experiment the β-phase remained stable during rapid quenching in the diamond anvil cell, which hinder synthesis of *Amm*2 and *Cmc*2_1-phases.

The calculated phase diagram also shows stability of *C*2/*m*-phase over the entire pressure-temperature range of the inner core, which highlight importance of this phase for the chemistry of the Earth's core.

3.2 Iron carbide Fe_7C_3

Both structure prediction methods revealed the well-known h-Fe_7C_3 as the most favorable phase in the range of 100–400 GPa. A similar result using the USPEX method was obtained by Bazhanova *et al.*[20] With AIRSS method, the h-phase was not found and the most favorable among predicted structures was *Cmc*2_1.[34] A comparison of *Cmc*2_1-structures of Fe_7C_3 and Fe_7N_3 shows their isostructural character, confirming crystallochemical similarity of carbon and nitrogen compounds at high pressures. Accordingly, we made the assumption about existence of Fe_7C_3-*C*2/*m* isostructural to Fe_7N_3-*C*2/*m*. The calculations of the enthalpies for Fe_7C_3-*C*2/*m*, indeed, confirmed both dynamic (Fig. S2 in the ESI†) and thermodynamic stability of this phase (Fig. 2b). According to these calculations h-Fe_7C_3 will transform into Fe_7C_3-*C*2/*m* at 366 GPa at 0 K. The calculation of Gibbs free energies indicate expanded stability of *C*2/*m* at the high-temperatures (Fig. 3b), and at 366 GPa Fe_7C_3-*C*2/*m* appears to be the most stable in the entire temperature range. At the pressures of the inner core boundary, 329 GPa, Fe_7C_3-*C*2/*m* becomes more favorable than h-Fe_7C_3 at temperature of ~1500 K.

3.3 Carbon–nitrogen content in the inner core

We calculated the density of the predicted Fe_7N_3-*C*2/*m* and Fe_7C_3-*C*2/*m* phases in the pressure range of 250–360 GPa and compared them with those of the Earth's inner core (Fig. 4). The density of the Fe_7N_3-*C*2/*m* and Fe_7C_3-*C*2/*m* is about 11% and 9% lower than those of hcp-Fe, respectively. If we assume that the core density deficit is compensated by the Fe_7N_3-*C*2/*m* phase, then its amount in the inner core is 30.9–42.7 wt% at 5000–6000 K. The same values for Fe_7C_3-*C*2/*m* are 28.3–38.9 wt%. The nitrogen and carbon content at such concentrations of nitride and carbide in the inner core will be 2.8–4.1 wt% and 2.2–3.3 wt%, respectively (Table 2).

4. Conclusions

As the result of the first-principle study of Fe_7N_3 and Fe_7C_3, we revealed new phases to be stable at Earth's core pressures. Fe_7N_3-*Cmc*2_1 is relatively low temperature phase and cannot be observed within the Earth's interiors, while the Fe_7N_3-*C*2/*m* is the only stable phase of this composition above 300 GPa through the entire temperature range. Isostructural phase of the carbide Fe_7C_3-*C*2/*m* has similar stability field with Fe_7N_3-*C*2/*m* in the pressure-temperature range of the inner core. This gives the base for the consideration of *C*2/*m*-phases of Fe_7C_3 and Fe_7N_3 as the possible hosts of carbon and nitrogen within Earth's core. The found similarity of the carbide and nitride *P*–*T* diagrams confirms crystallochemical similarity of carbon and nitrogen compounds and possible isomorphism between them.

Conflicts of interest

There are no conflicts to declare.

Acknowledgements

We thank Prof Chris Pickard for his help with AIRSS code. We are grateful to the Supercomputer Center, Novosibirsk State University, for access to the resources of the cluster. This work was supported by the Russian Science Foundation (project no. 17-17-01177).

Notes and references

1 T. Sakai, S. Takahashi, N. Nishitani, I. Mashino, E. Ohtani and N. Hirao, *Phys. Earth Planet. Inter.*, 2014, **228**, 114–126.
2 K. Litasov and A. Shatskiy, *Russ. Geol. Geophys.*, 2016, **57**, 22–46.
3 K. D. Litasov, I. S. Sharygin, P. I. Dorogokupets, A. Shatskiy, P. N. Gavryushkin, T. S. Sokolova, E. Ohtani, J. Li and K. Funakoshi, *J. Geophys. Res.: Solid Earth*, 2013, **118**, 5274–5284.
4 B. J. Wood, *Earth Planet. Sci. Lett.*, 1993, **117**, 593–607.
5 A. M. Dziewonski and D. L. Anderson, *Phys. Earth Planet. Inter.*, 1981, **25**, 297–356.

6 V. Busigny and G. E. Bebout, *Elements*, 2013, **9**, 353–358.
7 M. M. Grady and I. P. Wright, *Space Sci. Rev.*, 2003, **106**, 231–248.
8 N. Sugiura, *Meteorit. Planet. Sci.*, 1998, **33**, 393–409.
9 F. Kaminsky and R. Wirth, *Am. Mineral.*, 2017, **102**, 1667–1676.
10 B. Chen, L. Gao, B. Lavina, P. Dera, E. E. Alp, J. Zhao and J. Li, *Geophys. Res. Lett.*, 2012, **39**, L18301.
11 Y. Nakajima, E. Takahashi, N. Sata, Y. Nishihara, K. Hirose, K.-i. Funakoshi and Y. Ohishi, *Am. Mineral.*, 2011, **96**, 1158–1165.
12 B. Chen, Z. Li, D. Zhang, J. Liu, M. Y. Hu, J. Zhao, W. Bi, E. E. Alp, Y. Xiao and P. Chow, *Proc. Natl. Acad. Sci. U.S.A.*, 2014, **111**, 17755–17758.
13 J. F. Adler and Q. Williams, *J. Geophys. Res.: Solid Earth*, 2005, **110**, B01203.
14 S. Minobe, Y. Nakajima, K. Hirose and Y. Ohishi, *Geophys. Res. Lett.*, 2015, **42**, 5206–5211.
15 C. Prescher, L. Dubrovinsky, E. Bykova, I. Kupenko, K. Glazyrin, A. Kantor, C. McCammon, M. Mookherjee, Y. Nakajima and N. Miyajima, *Nat. Geosci.*, 2015, **8**, 220.
16 Z. Raza, N. Shulumba, N. M. Caffrey, L. Dubrovinsky and I. A. Abrikosov, *Phys. Rev. B: Condens. Matter Mater. Phys.*, 2015, **91**, 214112.
17 T. Das, S. Chatterjee, S. Ghosh and T. Saha-Dasgupta, *Geophys. Res. Lett.*, 2017, **44**, 8776–8784.
18 M. Mookherjee, Y. Nakajima, G. Steinle-Neumann, K. Glazyrin, X. Wu, L. Dubrovinsky, C. McCammon and A. Chumakov, *J. Geophys. Res.: Solid Earth*, 2011, **116**, B04201.
19 Y. Li, L. Vočadlo, J. Brodholt and I. Wood, *J. Geophys. Res.: Solid Earth*, 2016, **121**, 5828–5837.
20 Z. G. Bazhanova, A. R. Oganov and O. Gianola, *Phys.-Usp.*, 2012, **55**, 489–497.
21 K. Litasov, A. Shatskiy, S. Ovchinnikov, Z. Popov, D. Ponomarev and E. Ohtani, *JETP Lett.*, 2014, **98**, 805–808.
22 K. Litasov, A. Shatskiy, D. Ponomarev and P. Gavryushkin, *J. Geophys. Res.: Solid Earth*, 2017, **122**, 3574–3584.
23 P. Gavryushkin, N. Sagatov, Z. Popov, A. Bekhtenova, T. Inerbaev and K. Litasov, *JETP Lett.*, 2018, **107**, 379–383.
24 C. W. Glass, A. R. Oganov and N. Hansen, *Comput. Phys. Commun.*, 2006, **175**, 713–720.
25 A. R. Oganov and C. W. Glass, *J. Chem. Phys.*, 2006, **124**, 244704.
26 A. O. Lyakhov, A. R. Oganov and M. Valle, *Comput. Phys. Commun.*, 2010, **181**, 1623–1632.
27 A. O. Lyakhov, A. R. Oganov, H. T. Stokes and Q. Zhu, *Comput. Phys. Commun.*, 2013, **184**, 1172–1182.
28 C. J. Pickard and R. Needs, *Phys. Rev. Lett.*, 2006, **97**, 045504.
29 C. J. Pickard and R. Needs, *J. Phys.: Condens. Matter*, 2011, **23**, 053201.
30 C. J. Pickard and R. J. Needs, *Phys. Rev. B: Condens. Matter Mater. Phys.*, 2015, **91**, 104101.
31 P. N. Gavryushkin, N. S. Martirosyan, T. M. Inerbaev, Z. I. Popov, S. V. Rashchenko, A. Y. Likhacheva, S. S. Lobanov, A. F. Goncharov, V. B. Prakapenka and K. D. Litasov, *Cryst. Growth Des.*, 2017, **17**, 6291–6296.
32 D. Smith, K. V. Lawler, M. Martinez-Canales, A. W. Daykin, Z. Fussell, G. A. Smith, C. Childs, J. S. Smith, C. J. Pickard and A. Salamat, *Phys. Rev. Mater.*, 2018, **2**, 013605.
33 A. R. Oganov, C. W. Glass and S. Ono, *Earth Planet. Sci. Lett.*, 2006, **241**, 95–103.
34 G. L. Weerasinghe, R. Needs and C. J. Pickard, *Phys. Rev. B: Condens. Matter Mater. Phys.*, 2011, **84**, 174110.
35 G. Kresse, *Comput. Mater. Sci.*, 1996, **6**, 15.
36 G. Kresse and J. Furthmüller, *Phys. Rev. B: Condens. Matter Mater. Phys.*, 1996, **54**, 11169.
37 G. Kresse and D. Joubert, *Phys. Rev. B: Condens. Matter Mater. Phys.*, 1999, **59**, 1758.
38 J. P. Perdew, K. Burke and M. Ernzerhof, *Phys. Rev. Lett.*, 1996, **77**, 3865.
39 H. J. Monkhorst and J. D. Pack, *Phys. Rev. B: Solid State*, 1976, **13**, 5188.
40 M. Methfessel and A. Paxton, *Phys. Rev. B: Condens. Matter Mater. Phys.*, 1989, **40**, 3616.
41 A. Togo and I. Tanaka, *Scr. Mater.*, 2015, **108**, 1–5.